



RESEARCH

Open Access

Ultra-structural mapping of sugarcane bagasse after oxalic acid fiber expansion (OAFEX) and ethanol production by *Candida shehatae* and *Saccharomyces cerevisiae*

Anuj K Chandel^{1*}, Felipe F A Antunes¹, Virgilio Anjos², Maria J V Bell², Leonarde N Rodrigues², Om V Singh³, Carlos A Rosa⁴, Fernando C Pagnocca⁵ and Silvio S da Silva^{1*}

Abstract

Background: Diminishing supplies of fossil fuels and oil spills are rousing to explore the alternative sources of energy that can be produced from non-food/feed-based substrates. Due to its abundance, sugarcane bagasse (SB) could be a model substrate for the second-generation biofuel cellulosic ethanol. However, the efficient bioconversion of SB remains a challenge for the commercial production of cellulosic ethanol. We hypothesized that oxalic-acid-mediated thermochemical pretreatment (OAFEX) would overcome the native recalcitrance of SB by enhancing the cellulase amenability toward the embedded cellulosic microfibrils.

Results: OAFEX treatment revealed the solubilization of hemicellulose releasing sugars (12.56 g/l xylose and 1.85 g/l glucose), leaving cellulignin in an accessible form for enzymatic hydrolysis. The highest hydrolytic efficiency (66.51%) of cellulignin was achieved by enzymatic hydrolysis (Celluclast 1.5 L and Novozym 188). The ultrastructure characterization of SB using scanning electron microscopy (SEM), atomic force microscopy (AFM), Raman spectroscopy, Fourier transform–near infrared spectroscopy (FT-NIR), Fourier transform infrared spectroscopy (FTIR), and X-ray diffraction (XRD) revealed structural differences before and after OAFEX treatment with enzymatic hydrolysis. Furthermore, fermentation mediated by *C. shehatae* UFMG HM52.2 and *S. cerevisiae* 174 showed fuel ethanol production from detoxified acid (3.2 g/l, yield 0.353 g/g; 0.52 g/l, yield, 0.246 g/g) and enzymatic hydrolysates (4.83 g/l, yield, 0.28 g/g; 6.6 g/l, yield 0.46 g/g).

Conclusions: OAFEX treatment revealed marked hemicellulose degradation, improving the cellulases' ability to access the cellulignin and release fermentable sugars from the pretreated substrate. The ultrastructure of SB after OAFEX and enzymatic hydrolysis of cellulignin established thorough insights at the molecular level.

Background

Multidimensional applications have increased the demand for fossil fuels, sending disturbing signals regarding low levels of crude oil underground and the burden on aging refineries [1]. Recent developments have explored marginally meaningful alternatives to fossil fuels such as bioethanol using corn grains or sugarcane juice as substrates, which would result in tremendous price hikes for basic food commodities around the world [2]. However,

bioethanol produced from sustainable feedstocks such as lignocellulosics has drawn worldwide attention as a legitimate alternative to gasoline. The development of green gasoline or ethanol from abundantly available cellulosic materials in nature is gaining significant momentum as a sustainable mitigation strategy [3]. As an alternative to fossil and food-based fuels, cellulosic ethanol offers near-term environmental sustainability benefits. However, the selection of a raw substrate and its efficient utilization are critical steps in the process of economization. Brazil and India are the largest producers of sugarcane, with an annual production of about 650 and 350 MMT/year respectively [4], able to supply sugarcane bagasse (SB) in abundance round the year.

* Correspondence: anuj.kumar.chandel@gmail.com; silvio@debiq.eel.usp.br

¹Department of Biotechnology, University of São Paulo, School of Engineering of Lorena, Estrada Municipal do Campinho- Caixa, Postal 116 12.602.810, Lorena/SP, Brazil

Full list of author information is available at the end of the article

SB consists of crystalline cellulose nanofibrils embedded in an amorphous matrix of cross-linked lignin and hemicelluloses that impairs enzyme and microbial accessibility [5]. Structural changes in the cellular components of SB have been studied after pretreatment with formic acid [6], sono-assisted acid hydrolysis [7], and sequential acid–base [8] methodologies. However, visual characterizations of cellular components elucidating the hemicellulose degradation and delocalization of lignin after oxalic acid fiber expansion (OAFEX) pretreatment have yet to be performed. Cell wall anatomy of SB and macroscopic/microscopic barriers for cellulase-mediated saccharification reveal that cell wall hydrolysis encompasses several orders of magnitude (10^0 - 10^{-9} meters [9,10]).

Oxalic acid (OA) is a strong dicarboxylic acid with higher catalytic efficiency than the sulfuric acid, and acts primarily upon hemicellulose. Pretreatment with OA leaves cellulignin in a fragile form, making it amenable to concerted cellulolytic enzyme action on cellulose, which yields glucose. The current pretreatment methodologies used to degrade the holocellulosic (cellulose + hemicellulose) fraction of the plant cell wall have economic and environmental limitations. However, OAFEX has been found to be an efficient pretreatment strategy for hemicellulose removal from giant reed [11], *Saccharum spontaneum* [12], corn-cobs [13], and wood chips [14]. Therefore, a comprehensive structural analysis of the nanoscale architecture of OAFEX-treated cell walls in tandem with molecular changes will assist to explore the fundamental mechanisms of biomass recalcitrance.

The fermentation of pentose and hexose sugars present in lignocellulose hydrolysate is important to produce “economic ethanol” [15,16]. *Candida shehatae*, native xylose-fermenting yeast, has shown the capability to utilize pentose sugars efficiently for ethanol production [17,18]. The microorganism *Saccharomyces cerevisiae* is a perennial choice for bioethanol production from glucose-rich cellulosic hydrolysates [19]. We attempted to pretreat SB using OA followed by enzymatic hydrolysis. The released sugars (12.56 g/l xylose and 1.85 g/l glucose) were then subjected to ethanol fermentation using *C. shehatae* UFMG HM 52.2 and *S. cerevisiae* 174 in batch fermentation. A multiscale structural analysis of native, OAFEX-treated and enzyme-digested SB was performed using scanning electron microscopy (SEM), atomic force microscopy (AFM), X-ray diffraction (XRD), Raman spectroscopy, near infrared spectroscopy (NIR), and Fourier transform infrared (FTIR) analysis, and revealed the structural differences before and after OAFEX treatment and enzymatic hydrolysis.

Results and discussion

The abundance availability of SB as substrate can be used for fuel ethanol production without jeopardizing food and feed production. SB is rich in lignocellulosics

contained (% d. wt.): cellulose 45.0, hemicellulose 25.8, lignin 19.1, structural ash 1.0, extractive 9.1 [20]. The holocellulosic (hemicellulose + cellulose) content of SB (circa 70%) is fairly comparable with other lignocellulosic materials studied for ethanol production, such as wheat straw (54%), birch (73%), spruce (63.2%) (11), corn stover (59.9%), and poplar (58.2%) [21]. Biomass recalcitrance and efficient sugar conversion into ethanol are among the key hindrances to ethanol production that are preventing biorefineries from taking a central role in the energy sector.

OAFEX treatment of sugarcane bagasse and detoxification of hemicellulosic hydrolysate

OA is a strong organic acid, and due to its di-carboxylic properties, is better for hemicellulose hydrolysis than mineral acids such as sulfuric or hydrochloric acid [13]. OAFEX pretreatment is known for its precise action to degrade hemicellulose with fewer inhibitors and increased surface area of cellulose for improved enzymatic action [11,13,14,22,23]. The dilute OA hydrolysis of SB (160°C; 3.5% OA w/v; 10% total solids; 20 min residence time) depolymerized the hemicellulose fraction of the bagasse cell wall into sugars (xylose 12.56 g/l, glucose 1.85 g/l, arabinose 0.85 g/l) with the hemicellulose conversion (90.45%) and inhibitors (0.234 g/l furfurals, 0.103 g/l 5-hydroxy methyl furfural (5-HMF), 1.47 g/l acetic acid and 2.95 g/l total phenolics) (Table 1). Diluted OA hydrolysis degrades the hemicellulosic fraction of the plant cell wall into its monomeric constituents, such as xylose and other sugars, in addition to inhibitory compounds [13,22].

After hemicellulose is removed from the substrate during the OAFEX treatment, the leftover solid material, called cellulignin, becomes accessible for enzymatic saccharification. Critical factors such as lignocellulosic substrate, temperature, acid load, residence time, and substrate-to-liquid ratio play key roles in breaking down hemicellulose into its monomeric constituents [13,14], in addition to releasing inhibitors from the substrate [17]. Scordia et al. [12] reported 30.70 g/L xylose (93.73% conversion), 2.60 g/L glucose (54.17% conversion), 1.40 g/L arabinose, 3.60 g/L acetic acid, 0.68 g/L furfurals, 0.10 g/L HMF, and 6.58 g/L phenolics from *S. spontaneum* under the hydrolytic conditions (158°C, 16 min, 3.21% w/w OA, solid-to-liquid ratio of 1:4). The OA-mediated hydrolysis of giant reed (*Arundo donax* L.) revealed 100% recovery of xylose, arabinose, glucose, 6.55 g/L furfural, and 0.18 g/L HMF at defined hydrolysis conditions, i.e. 190°C, 25 min, 5% w/w OA [11]. Maize residues pretreated with OA (160°C, 1.8% OA, 10 min residential time) showed 28±2.5% w/w xylose yield [23]. These studies reveal the potential of OA pretreatment for hemicellulose degradation into fermentable sugars.

Table 1 Sugarcane bagasse hemicellulosic hydrolysate profile after detoxification by calcium hydroxide overliming

Constituents	Quantity (g/l)	% Reduction after overliming	Residual constituents quantity (g/l)
Xylose	12.56	7.51	11.61
Glucose	1.85	25.50	1.37
Arabinose	0.85	8.56	0.777
Acetic acid	1.47	5.54	1.38
Furfural	0.242	23.96	0.184
5-HMF	0.094	10.63	0.084
Total phenolics	2.95	45.5	1.60

The values are mean of three replicates. Standard deviation was within 10%.

Fermentative inhibitors are common in acidic hydrolysis of SB. OA hydrolysate can be detoxified effectively using calcium hydroxide overliming: raising the pH of hydrolysate to 10.0. Regardless the source of availability of lignocellulosic hydrolysate, the detoxification using calcium hydroxide overliming is tedious and a subject of further investigation. It is an intensive step which cause precipitation and stirring problems. The re-adjustment to pH 6.0 showed efficient removal of inhibitors from the hydrolysate (Table 1). After $\text{Ca}(\text{OH})_2$ overliming of the SB hemicellulosic hydrolysate, a significant reduction in furfurals (23.96%), 5-HMF (10.63%), total phenolics (45.5%), and acetic acid (5.54%) was observed with a marginal loss in xylose (7.51%), glucose (25.50%), and arabinose (8.56%) (Table 1). During $\text{Ca}(\text{OH})_2$ overliming at pH 10, precipitation of furfurals and phenolics occurs, resulting in their removal during vacuum filtration of the hydrolysate. Earlier, we have reported 41.75% and 33.21% reductions in furans and phenolics from *S. spontaneum* hemicellulosic hydrolysates after $\text{Ca}(\text{OH})_2$ overliming [24]. There was only a 5.5% reduction in acetic acid content after overliming. In another study, Rodrigues et al. [22] observed no change in acetic acid concentration after overliming of corn stover hemicellulosic hydrolysate.

Enzymatic hydrolysis

OAFEX-treated bagasse was enzymatically hydrolyzed with commercial enzymes, i.e., 20 FPU/g of Celluclast 1.5 L and 30 IU/g of Novozym 188 at 50°C for 96 h in the presence of tween-20. Enzymatic hydrolysis after 72 h revealed 28.5 g/L glucose release with 66.51% saccharification efficiency (Figure 1). The OAFEX-treated bagasse showed a concomitant increase in sugar recovery up to 72 h followed by a decrease in glucose concentration at 96 h of incubation. These enzyme loadings in the presence of surfactants are sufficient to hydrolyse the cellulose present in pretreated substrate.

A similar trend was reported in the sugar recovery during enzymatic hydrolysis of aqueous-ammonia-pretreated *S. spontaneum* [25]. The amounts of enzymes required for hydrolysis of pretreated raw material depend upon the pretreatment applied to the substrate and the availability of carbohydrate content in the substrate [26]. A maximum

yield of sugars (482 ± 22 mg/g, 64% hydrolytic efficiency) from acidic-hydrolyzed wheat straw (7.83% DS, acid loading 0.75%) was obtained after enzymatic hydrolysis [26]. We also observed 28.5 g/l glucose representing 66.51% efficiency after enzymatic hydrolysis of OAFEX-treated bagasse in the presence of tween-20 (2.5 g/l). Zheng et al. [27] observed that high enzyme loadings did not alter saccharification and yields. Rezende et al. [8] reported 72% cellulose conversion from consecutive acid–base pretreated SB. A 65% cellulose conversion was obtained after the enzymatic hydrolysis (1.91% w/w pretreated SB, 20 FPU/g enzyme loading, 0.05 g/g surfactant) of bagasse pretreated with dilute sulfuric acid (1.75% w/w bagasse content, 1.7% w/w H_2SO_4 loading, 150°C, and 30 min pretreatment time) [20]. Our results indicate that hemicellulose removal and the possible relocation of lignin moieties during OAFEX treatment could yield the desired amount of sugar toward the goal of developing an intensified and simplified process for cellulose saccharification.

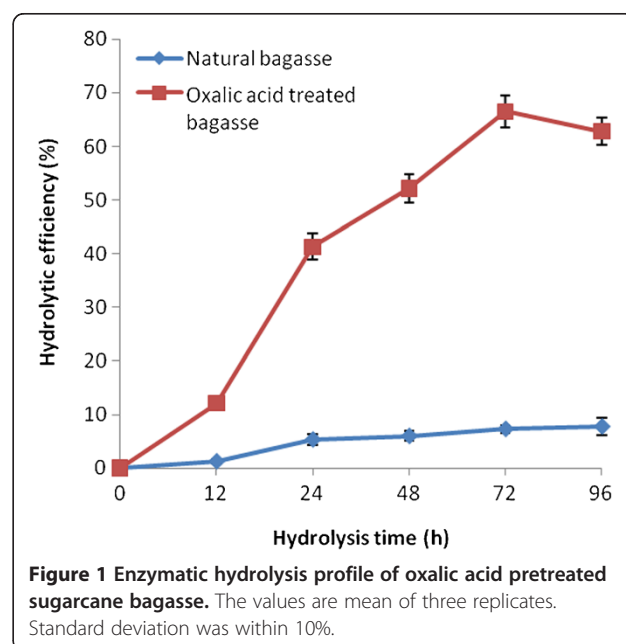


Figure 1 Enzymatic hydrolysis profile of oxalic acid pretreated sugarcane bagasse. The values are mean of three replicates. Standard deviation was within 10%.

Ultra structural characterization of native and treated SB

SB, the biomass is naturally built through a special arrangement of cross-linked lignin with a holocellulose network, providing a superb mechanism to protect itself from microbial invasions in nature [5]. Rendering the carbohydrate fraction of the cell wall accessible is a multiscale phenomenon encompassing several orders of magnitude due to both macroscopic (compositional heterogeneity, mass transfer limitations) and microscopic barriers (holocellulose crystallinity, lignin-cellulose linkage) [28]. The pretreatment allows cellular breakdown, increasing the amenability of enzymes for sugar monomer recovery. The SEM and AFM of cell walls after acidic treatment reveal disorganization of cell wall components, which is pivotal for improved cellulase action on the carbohydrate polymer in order to yield simple sugars.

Cell wall composition

A physico-chemical analysis of the native SB cell wall revealed a composition (dry weight) of 24.67% total lignin (20.88% Klason lignin + 3.79% acid soluble lignin), 41.22% cellulose, 25.62% hemicellulose, 2.90% extractives, 8.16% moisture, and 1.5% structural ash. This composition of SB is in agreement with earlier studies [20]. The treated substrate after OA pretreatment of SB revealed 58.84% cellulose, 8.75% hemicellulose, and 24.56% total lignin (24.18% Klason lignin + 0.38% acid soluble lignin). The total lignin content in natural and OA-pretreated bagasse was determined to be almost similar (OA: 24.56%; natural: 24.67%). Klason lignin content increased in the OA-treated bagasse (24.18%) compared to the native bagasse (20.88%). However, acid-soluble lignin was removed maximally in the OA-pretreated bagasse, making the total content almost similar.

The pretreatment of corn cob with OA showed 100% removal of hemicellulose with a partial increase in lignin. Lee et al. [13] observed 6.76% xylan, 35.09% glucan, 0.12% galactan, 0.55% arabinan, and 12.09% lignin in OA-pretreated corn cob (168°C, 26 min, 30 g/l OA, 1:6 solid-to-liquid ratio) compared with the native material (27.86% xylan, 37.07% glucan, 0.61% galactan, 2.19% arabinan, and 13.92% lignin). The changes in cell wall composition of lignocellulosic material after OA pretreatment depend upon the nature of the substrate and the conditions explored during pretreatment [11-13].

Scanning electron microscopy (SEM)

SEM analysis indicated the cell wall degradation, and surface properties of native, OA-pretreated, and enzymatically digested SB (Figure 2a-c). The native SB cell wall showed parallel stripes and waxes, extractives, and other deposits on the surface (Figure 2a). Obtained results are in agreement with earlier studies, where OA was reported to disrupt the structure of fibers and pith by removing the

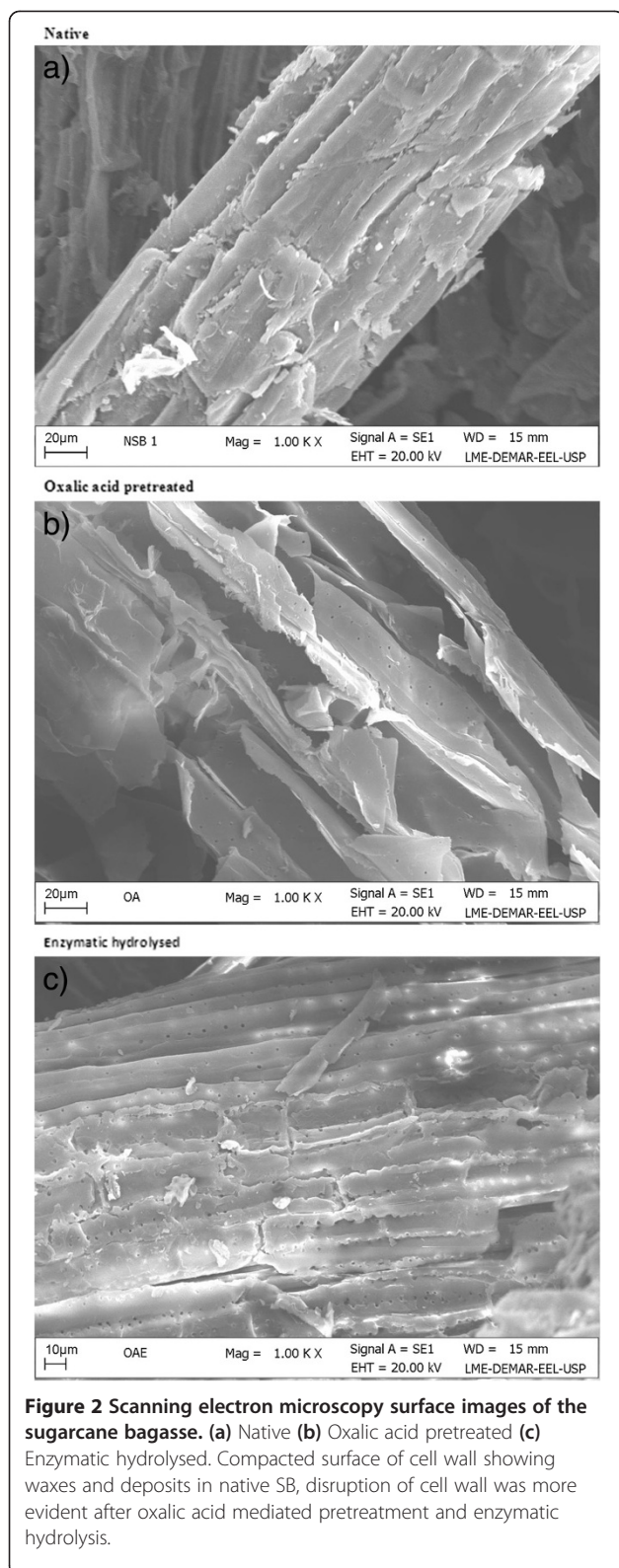
hemicellulose fraction of the cell wall, waxes, and other deposits. OAFEX leaves the overall structure disorganized, simultaneously increasing the surface area for enzymatic action [14,23].

OA-pretreated bagasse fiber showed small pores on the surface and fiber disruption, which revealed the efficacy of the pretreatment process (Figure 2b). The OAFEX-treated SB revealed disruption of cell wall after enzymatic hydrolysis. Similarly, Rezende et al. [8] observed a disrupted fiber surface and exposed parallel stripes after sulfuric acid pretreatment of SB. Our data is in agreement and indicates severe disruption and exposure of parallel stripes in OAFEX-treated SB (Figure 2b). After the enzyme treatment of SB, the analysis showed maximum disintegration and numerous holes in the cell wall, verifying the enzymatic action on cellulose (Figure 2c). The exposure of cellulose through structural alteration of the bagasse is the crucial factor in hydrolysis of the remaining cellulosic fraction present in the cell wall. Similar observations have been reported from enzymatic hydrolysis of dilute-sulfuric-acid-pretreated *S. spontaneum* [24,25]. Kristensen et al. [29] also observed similar effect on wheat straw cell walls after hydrothermal pretreatment.

Atomic force microscopy (AFM)

Amplitude and phase images were captured to show the changes in secondary cell walls and thickened vascular bundle cell surfaces of native, OAFEX-treated, and enzymatically digested SB (Figure 3a-c). The native SB showed a fibrous network of cellulose, cross-linked lignin, and hemicellulose in the parenchyma of the primary wall (Figure 2a), which is also shown by the AFM image, intact with a uniform surface (Figure 3a). The native SB surface was predominantly hydrophobic (95.40 nm), as confirmed by the darker phase image (Figure 3a). OA specifically disrupts hemicellulose, retaining cellulose and lignin together. The OAFEX-treated SB clearly showed the non-homogeneous phase and globular surface deposition in the amplitude phase (Figure 3b). The AFM tip showed increased affinity toward hydrophilic regions (192 nm) that appear light in color due to a significant change in phase image (Figure 3b). The surface of OA-treated SB is non-uniform, encompassing irregularly shaped hydrophilic deposits, probably due to the exposure of cellulose. Chundawat et al. [28] observed similar patterns in corn stover after pretreatment with ammonium hydroxide.

The presence of globular and irregular shapes (20–95 nm in diameter) can be characteristic of lignin deposits in the cell wall (Figure 3b). This interpretation is in accordance with the SEM analysis, where re-localization of lignin is apparent, linking with cellulose lamellae/agglomerates (Figure 2b). Lignin re-localization is an important feature that may lead to enhanced enzymatic hydrolysis. OA markedly disrupts hemicellulose and simultaneously



re-localizes lignin moieties, aiding the increased exposure of cellulose to cellulases [29,30].

The higher-resolution imaging of AFM reveals maximum non-uniformity in the cellulose lamellae, which can be interpreted as the complete disruption of cellulose aggregates into glucose (Figure 3c). The AFM tip showed high affinity toward hydrophilic areas (192 nm) appearing as changes in phase, and the light color shows the effective accessibility of cellulose to cellulases. Igarashi et al. [31] reported that the real-time visualization of cellulase from *Trichoderma reesei* cellobiohydrolase I action on crystalline cellulose resulted in marked cellulase affinity toward cellulose.

X-ray diffraction (XRD)

XRD analysis revealed the increasing order of crystallinity index (CrI) in OAFEX-treated bagasse (52.56%) and enzyme-digested bagasse (55.65%) compared to native bagasse (45.61%). Figure 4 shows the XRD spectra of native, OAFEX-treated, and enzyme-digested bagasse. In general, after pretreatment of SB, CrI increases with the decrease of amorphous regions in the substrate along with other constituents [6]. The CrI of OAFEX-treated bagasse increases mainly due to removal of hemicellulose in conjunction with re-localisation of lignin and partial disruption of cellulose. Rezende et al. [8] reported that the CrI of consequentially acid–base-pretreated SB increased with a parallel increase in the amount of cellulose in the substrate. Velmurugan and Muthukumar [7] observed a high CrI in sono-assisted alkali-pretreated SB (66%) compared with natural bagasse (50%). The increase in CrI of OAFEX-treated bagasse and enzyme-digested bagasse was due to the depolymerization of hemicellulose and cellulose into their monomeric constituents. Cellulase enzyme cocktails break down the amorphous cellulose, thus increasing the CrI over OAFEX-treated bagasse. However, cellulose crystallinity is not considered to be a principal factor that determines biomass recalcitrance [8].

Raman spectroscopy

Raman spectroscopic analysis revealed a gradual reduction in the band intensity ($< 1500 \text{ cm}^{-1}$) in OAFEX-treated and enzymatically hydrolyzed SB compared to the native bagasse (Figure 5). The molecular disarrangement and displacement in the hemicellulosic backbone during pretreatment followed by enzymatic cleavage of the β -1-4-glycosidic linkage of cellulose may have caused this gradual reduction in overall band intensities. Previous studies that performed Raman spectroscopic analysis of cellulose and hemicellulose showed that the changes in spectra were dominated by contributions from cellulose at intensities below 1500 cm^{-1} [32]. The ratio of the bands at 1172 cm^{-1} and 1204 cm^{-1} reflects the orientation of the cellulose relative to the electric vector (polarization) of the laser [33].

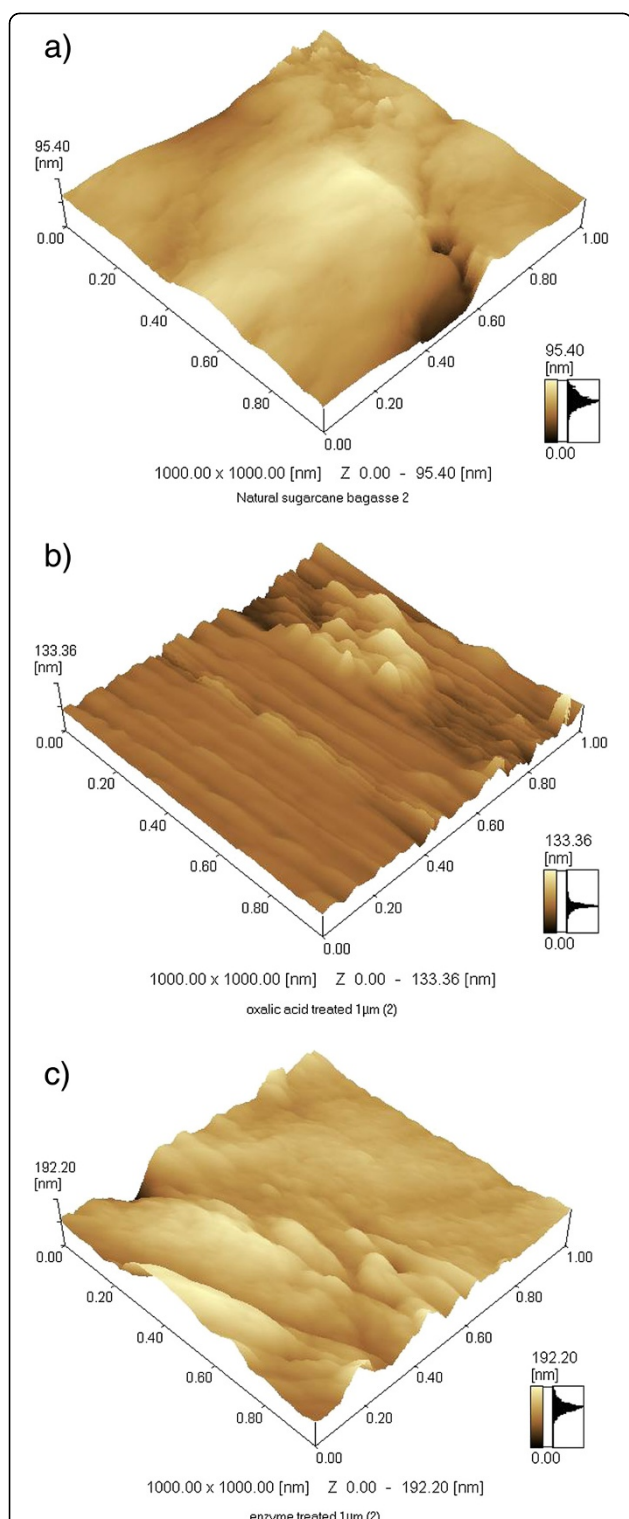


Figure 3 Atomic force microscopy (AFM) amplitude images. (a) Native sugarcane bagasse **(b)** Oxalic acid-pretreated bagasse **(c)** Enzyme hydrolysed bagasse. AFM scan revealed the cross linked cellulose + hemicellulose network in native SB. After OA pretreatment, non homogenous surface appeared with globular surface deposition (characteristic of lignin). AFM tip indicated affinity towards hydrophilic areas (192 nm) revealing the breakdown of cellulose.

In Raman analysis, the electric field vector has a component along the cellulose axis causing the intensification of the band at 1172 cm^{-1} , and considered to obtain the spectral analysis of native, OAFEX-treated, and enzyme-digested SB. Figure 5 shows cellulose/ hemicellulose peaks at 1088 and 1371 cm^{-1} . It is evident here that OA pretreatment and enzymatic hydrolysis act on hemicellulose and cellulose respectively. In addition, the main signature of lignin in all three samples is strong band lines at 1603 and 1630 cm^{-1} due to stretching of the asymmetric aryl ring in lignin [33,34]. This may be due to the re-localization of lignin moieties during OA pretreatment of SB at a high temperature. Ooi et al. [34] reported that Raman spectra of native and NaOH-treated Kenaf fibers showed a reduction in intensity of lignin bands in the region around 1750 cm^{-1} assigned to acetyl groups with the carbonyl, C=O group. No significant changes were observed in the intensities of lignin bands at 1750 cm^{-1} , maybe due to the fact that OA and enzymatic hydrolysis specifically act on hemicellulose and cellulose respectively.

Fourier transform infrared spectroscopy (FTIR)

FTIR spectroscopy was carried out to investigate the changes in hemicellulose and cellulose structure during OAFEX treatment and enzymatic hydrolysis. FTIR spectra of the native SB show a band at 900 cm^{-1} representing the β -(1-4) glycosidic linkages of cellulose (Figure 6a-d). The frequency range between 1200 – 1000 cm^{-1} has a large contribution of hemicellulose and cellulose with maxima at 1037 cm^{-1} due to C-O stretching mode and 1164 cm^{-1} due to the asymmetrical stretching C-O-C [35,36]. The absorption at 1247 cm^{-1} shows due to C-O stretching and is a feature of the hemicelluloses, as well as of lignin [37]. There is divergence about the region at 1316 cm^{-1} (Figure 6b), which can be attributed to vibration of the CH_2 group of cellulose [35]. Pandey attributes it to the C-O syringyl ring in lignin [38].

The absorption around 1463 cm^{-1} refers to CH_2 and CH_3 deformation of lignin, while 1606 cm^{-1} is related to C=C stretching of the aromatic ring (lignin) and C=O stretching (Figure 6c). The absorption around 1515 cm^{-1} is associated with C=C aromatic skeletal vibration [35,38]. The absorption in 1733 cm^{-1} is attributed to a C=O unconjugated stretching of hemicelluloses but also with the contribution of lignin [35,38]. The small peaks at 2850 cm^{-1} and 2918 cm^{-1} come from CH_2 and CH symmetric and asymmetric stretching respectively (Figure 6d). Both are characteristic of cellulose [36]. The obtained data agree that the range 3800 – 3000 cm^{-1} comprises bands related to the crystalline structure of cellulose [35]. The region is of great importance and is related to the sum of the valence vibrations of H-bonded OH and intramolecular and intermolecular hydrogen bonds. In the range 1300 – 1000 cm^{-1} , the appearance of

two peaks at 1033 cm^{-1} and 1058 cm^{-1} were observed in OAFEX-treated bagasse and enzyme-digested cellulignin spectra respectively (Figure 6b). This indicates penetration of OA in the amorphous region of the biomass and degrading hemicellulose.

Further, the removal of the hemicelluloses is clearly seen by comparing the band around 1247 cm^{-1} with the abrupt decrease of the same band in the OAFEX-treated bagasse (Figure 6b). In the range $1800\text{--}1400\text{ cm}^{-1}$, we did not observe changes except around 1733 cm^{-1} , which indicates chemical changes in hemicellulose and/or lignin (Figure 6c). Nevertheless, no apparent changes were observed in the lignin-characteristic bands around 1606 cm^{-1} , 1515 cm^{-1} and 1463 cm^{-1} . Therefore, it is reasonable to state that the hemicellulose was degraded by the action of the OA, which appears to be less stable than lignin. These observations could reflect that the lignin composed of percentages of p-hydroxyphenyl (H), guaiacyl (G), and syringyl (S) units is highly condensed and very resistant to degradation. Further, the $3000\text{--}2800\text{ cm}^{-1}$ range shows a decrease of two local maxima mainly in the enzyme-digested cellulignin, indicating the cellulose hydrolysis (Figure 6d).

FTIR spectroscopy, together with the deconvolution technique, provides distinct positions of the bands in this region. Gaussian distribution of the modes in the deconvolution process showed the three bands (Figure 7a-c). The band range from $3310\text{ to }3228\text{ cm}^{-1}$ refers to the intermolecular hydrogen bond $\text{O}(6)\text{H}\dots\text{O}(3)$ (Figure 7), $3375\text{ to }3335\text{ cm}^{-1}$ belongs to the intramolecular hydrogen bond $\text{O}(3)\text{H}\dots\text{O}(5)$, and $3460\text{ to }3410\text{ cm}^{-1}$ is related to the intramolecular hydrogen bond $\text{O}(2)\text{H}\dots\text{O}(6)$ (Figure 7). The band around 3585 cm^{-1} (band 1 in Figure 7) has been reported as the contribution of free hydroxyl [39].

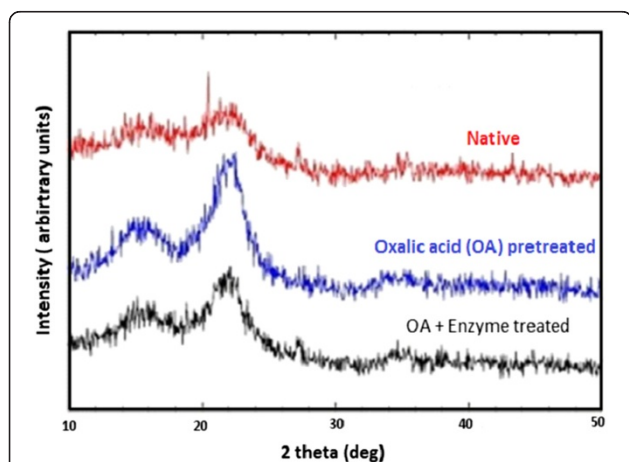


Figure 4 X-ray diffraction pattern of native, oxalic acid pretreated and enzyme hydrolysed SB. Crystallinity Index (Crl) was found to be increased in OA pretreated SB and enzymatic hydrolysed SB showing the effect of OAFEX and enzymatic degradation.

The deconvolution FTIR spectra reveal three bands of the crystalline structure of cellulose (Figure 7). Band 3 of intermolecular hydrogen bonds has shifted to a higher wave number (3220 cm^{-1} ; 3239 cm^{-1} ; 3246 cm^{-1}), revealing the depolymerization of crystalline cellulose (Figure 7b). Band 2 of intramolecular hydrogen bonds has also shifted to higher frequencies (3433 cm^{-1} ; 3443 cm^{-1} ; 3446 cm^{-1}) indicating the formation of intramolecular hydrogen bonds when OA penetrated the crystalline structure of cellulose (Figure 7c). This shift is evidence of an energy change in the internal interactions of cellulose [40,41]. The disruption of the structure of plant vegetal fibers and the removal of hemicellulose and/or lignin from the polymer matrix can also configure a closer relationship between the cellulose chains. Another indication of this behavior is the increase in the width and asymmetry of the curves for the OAFEX-treated bagasse.

Near infrared spectroscopy (NIR)

FT-NIR spectra of native, OAFEX-treated, and enzyme-digested SB ranged from $7200\text{ to }4000\text{ cm}^{-1}$ (Figure 8). The spectral region from $6000\text{ to }5920\text{ cm}^{-1}$ is assigned to the first overtone C-H stretching vibration of aromatics. This could be due to the re-localization of lignin moieties during OA-mediated pretreatment at a high temperature [42,43]. In regard to the hemicellulose structural change, the first overtone C-H stretch around 5800 cm^{-1} is responsible for

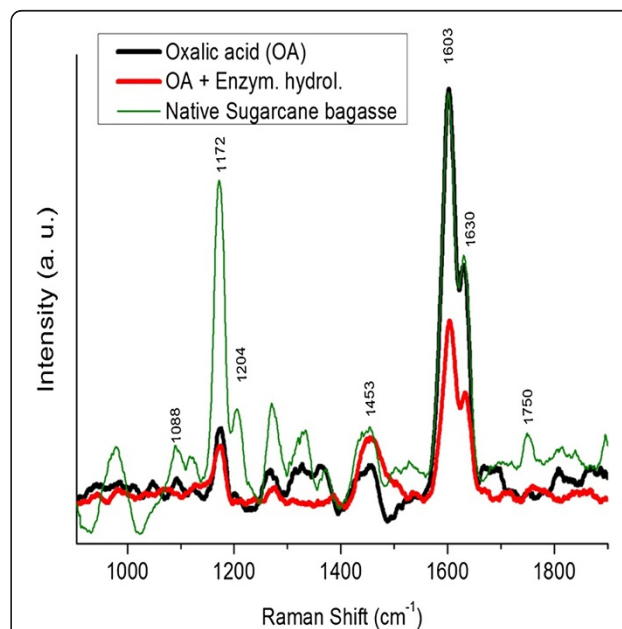


Figure 5 Raman spectra of native sugarcane bagasse (green online), pre-treated bagasse with oxalic acid (black online) and oxalic acid enzymatic hydrolysis pre-treated bagasse (red line). A gradual reduction in band intensities was recorded in OAFEX and enzymatic hydrolysis revealing the displacement in hemicellulose backbone and enzymatic cleavage of β -1-4-glycosidic linkage in cellulose.

its variation [42,44]. This reveals that the absorbance of the hemicellulose decreases with diminishing hemicellulosic content in SB. This drastic change in absorbance in hemicellulose is due to the severe pretreatment given to the SB [42].

The stressed regions (grey) around 7000 cm^{-1} correspond to amorphous cellulose (Figure 8). The spectral band around $6290 \pm 20\text{ cm}^{-1}$ is attributed to crystalline cellulose (CII) and the presence of polysaccharides is shown at 5400 to 4000 cm^{-1} [42,44]. Additionally, we observed changes in the polysaccharide content in the regions around 6300 , 5208 , 4813 , 4285 , and 4405 cm^{-1} . The amorphous region of polysaccharide around 7000 cm^{-1} had a small increase, suggesting the re-localization of lignin units [42].

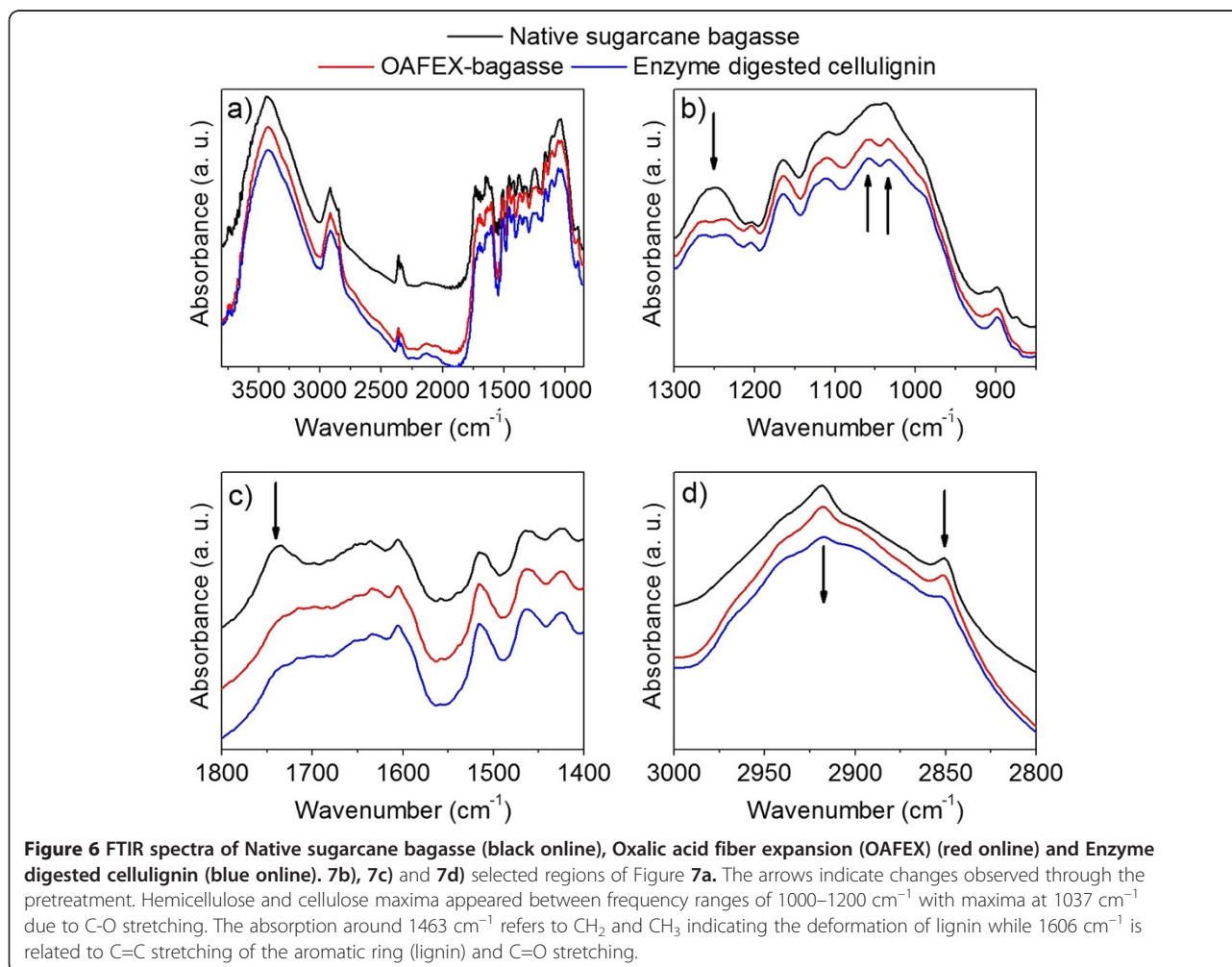
Ethanol fermentation

Detoxified hemicellulosic hydrolysate and enzymatic hydrolysates were used for ethanol production using yeasts *C. shehatae* UFMG52.2 and *S. cerevisiae* 174

under submerged culture cultivation. The microorganisms selected for bioconversion of ethanol have been established for the fermentation of xylose and glucose sugars for ethanol production [17,19].

Fermentation of acid hydrolysate

The fermentation profile of detoxified SB acid hydrolysate from *C. shehatae* UFMG52.2 and *S. cerevisiae* 174 in batch culture is shown in Figure 9a, b. The microorganism *C. shehatae* reached maximum ethanol production (3.20 g/l) with a yield of 0.353 g/g and productivity of 0.133 g/l/h from detoxified hemicellulosic acid hydrolysate after 24 h, and declined afterwards (Figure 9a). The biomass continued to increase even after 24h to the completion of the fermentation cycle (72 h), and yielded 0.385 g/g with productivity of 0.0496 g/l/h (Table 2). The detoxified hemicellulose hydrolysate did not show satisfactory ethanol production (Figure 9b) by *S. cerevisiae*, which suggests that the microorganism was unable to utilize the abundance of xylose sugar in the hydrolysate. After 72 h of incubation, a



biomass yield of 0.179 g/g and productivity of 0.011 g/l/h were observed (Table 2).

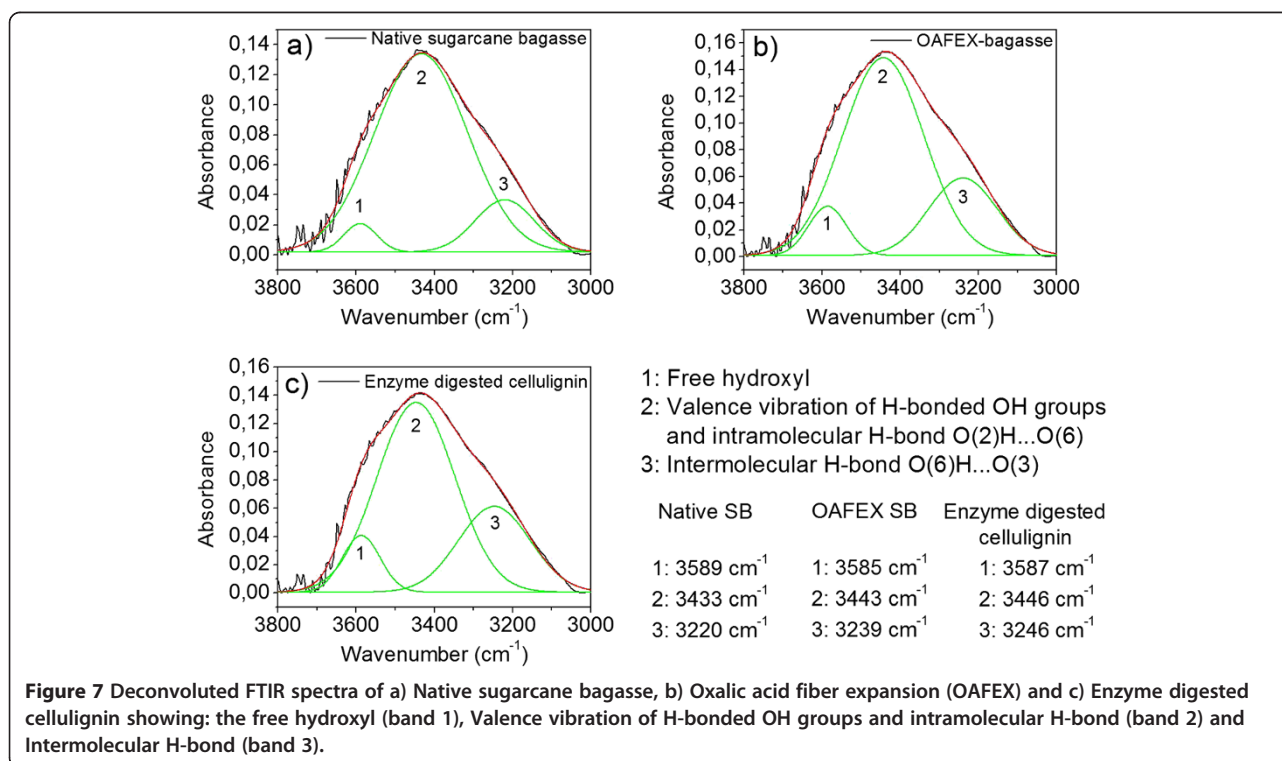
Fermentation of enzyme hydrolysate

When the enzymatic hydrolysate was fermented with *C. shehatae* UFMG52.2, maximum ethanol production (4.83 g/l) was found with a yield of 0.282 g/g and productivity of 0.201 g/l/h after 24 h (Figure 10a; Table 2). However, regular growth of microorganisms was observed until the sugar was consumed after 72 h. The maximum biomass production (6.32 g/l) was obtained with a yield of 0.302 g/g and productivity of 0.877 g/l/h. Fermentation of enzymatic hydrolysate with *S. cerevisiae* showed maximum ethanol production (6.6 g/l) after 24 h, with a yield of 0.46 g/g and productivity of 0.47 g/l/h after 14 h of incubation (Figure 10b). The growth in biomass remained unchanged until 72 h of incubation (Figure 10b; Table 2).

C. shehatae showed a greater ethanol yield (0.353 g/g) from the acid hydrolysate than from the enzymatic hydrolysate (0.282 g/g), indicating a microbial preference for xylose over glucose as a source of carbon in the fermentation reaction. However, *C. shehatae* is sensitive to fermentation inhibitors present in the hydrolysate. Sreenath et al. [45] showed ethanol production of 5 g/l with a yield of 0.25 g/g by *C. shehatae* FPL 702 from alfalfa hydrolysate. The low ethanol yield of this yeast was probably due to

inhibition by pectic acid, organic acids, and hemicellulose-derived inhibitors present in the sugar solution [45]. The hemicellulosic hydrolysates contain mainly xylose, while enzymatic hydrolysates contain only glucose. When *S. cerevisiae* was grown on hemicellulosic hydrolysate, abysmal ethanol production and growth were recorded (Table 2). *S. cerevisiae* does not use xylose present in the hemicellulosic hydrolysate, but rather relies upon glucose, which could be why the poor ethanol production was observed (Figure 9b). Our earlier studies showed that *S. spontaneum* acid hydrolysate after overliming fermented with *S. cerevisiae* VS₃ in batch conditions produced 1.40±0.07 g/l ethanol with 0.20±0.016 g/g yield after 36 h of fermentation [24].

C. shehatae showed a similar growth pattern in both the hydrolysates. In both cases, more than 80% of the sugars were utilized within 24 h of incubation promoting faster growth of microorganism. Similar patterns of biomass growth were observed by Abbi et al. [46], and Chandel et al. [17] reported a regular increase in biomass of *C. shehatae* NCIM 3501 after the exhaustion of xylose in 24 h with the utilization of ethanol as a carbon source for the metabolic growth. Sánchez et al. [47] observed ethanol production (4.5 g/L) from *C. shehatae* CBS4410 utilizing *Paja brava* acid hydrolysate (19.8 g/L xylose, 2.5 g/L glucose) obtained under hydrolysis conditions (180°C, 5 min, 0.5% w/w H₂SO₄). Sreenath and Jeffries [48] reported that *C. shehatae* FPL-Y-049 utilized all sugars



present in wood hemicellulose hydrolysate except arabinose and produced 34 g/L of ethanol with a yield of 0.46 g/g.

The fermentation of enzymatic hydrolysate (18.4 g/l glucose) by *S. cerevisiae* produced maximum ethanol (6.6 g/L, yield 0.46 g/g) after 14 h of incubation under conditions similar to those employed for hemicellulose hydrolysate fermentation (Figure 10b). It is interesting to note that both yeast strains isolated from Brazilian biodiversity presented a higher growth rate with a shorter lag phase and a prolonged exponential phase. The current growth pattern of both microorganisms supports maximal conversion of sugars into ethanol—an impressive trait for achieving higher ethanol productivity. These characteristics could be beneficial in biorefineries by saving time and reducing the cost of operation and energy.

The maximum ethanol productivity (0.47 g/l/h) was obtained from *S. cerevisiae*-mediated fermentation of OAFEX-treated SB enzymatic hydrolysate, another impressive feature of the *S. cerevisiae* strain used in this study (Table 2). Previously, a natural isolate from spent sulphite liquor, *S. cerevisiae* ATCC 96581, showed maximum ethanol production (7.4 g/l, yield 0.28 g/g and productivity 0.37 g/l/h) from detoxified SB hydrolysate containing 26.0 g/l total sugars [19]. Unlike acid hydrolysates, enzymatic hydrolysate lacks fermentative inhibitors, which eliminates the detoxification step. During the fermentation of enzymatic hydrolysate, *S. cerevisiae* showed less biomass production (4.03 g/l, yield 0.22 g/g) compared to *C. shehatae* (6.32 g/l, yield 0.302 g/g) after

72 h of incubation, suggesting that *C. shehatae* prefers to metabolize a carbon source for ethanol production rather than produce cellular buildup. However, the characteristic of selecting ethanol as a carbon source after the exhaustion of sugars was also observed in *S. cerevisiae* 174.

Conclusion

Plant cell walls are complex, rigid, and recalcitrant in nature. Pretreatment is an inevitable process to break down this carbohydrate skeleton and increase the accessibility of cellulose. Our studies indicated that OA-mediated hemicellulose degradation of SB is an effective pretreatment strategy that ameliorates the enzymatic hydrolysis of the cellulosic fraction into glucose. The microscopic and spectroscopic techniques used in this work warranted in-depth structural investigation of chemical changes at the molecular level during pretreatment and enzymatic digestion. OAFEX pretreatment significantly removed hemicellulose, causing lignin re-localization, which eventually showed efficient enzymatic action toward the depolymerization of cellulose into glucose (66.51% hydrolytic efficiency). Detoxified hemicellulosic hydrolysate, when fermented by *C. shehatae* UFMG52.2 and *S. cerevisiae* 174, showed ethanol production of 3.20 g/L (yield 0.353 g/g) and 0.52 g/L (yield 0.246 g/g) respectively. Enzymatic hydrolysate after fermentation with *C. shehatae* UFMG52.2 and *S. cerevisiae* 174 produced 4.83 g/L (yield 0.282 g/g) and 6.6 g/L (yield 0.46 g/g) respectively. Both microorganisms revealed high substrate consumption including energy and time savings that could have a major impact in biorefineries.

Material and methods

Preparation of raw substrate

The raw substrate, sugarcane bagasse, was acquired from Usina Vale do Rosário (Morro Agudo, S.P, Brazil). In preliminary processing, the SB was air-dried, and knife milled (Marconi Equipamentos, Model No. MA 680, Piracicaba-S.P, Brazil) to pass through with 20-mesh sieve. The finely milled bagasse was washed under running tap water to remove the dust, and dried at 45°C for further experiments.

Oxalic acid fiber expansion pretreatment of sugarcane bagasse

The pretreatment of the SB with dilute oxalic acid (OA) (3.5% w.v⁻¹) was carried out at 160°C for 20 min as described by Scordia et al. [12]. Briefly, SB (10 g d.wt.) and 100 ml (3.5% w.v⁻¹) aqueous OA solution (10% total solids) were loaded into a 200 ml stainless-steel container (19x9.7 cm), tightly sealed and immersed in an oil bath provided with electrical heating at 160°C. The container remains resident for 5 min to reach the temperature of 160°C. The hydrolysis was stopped

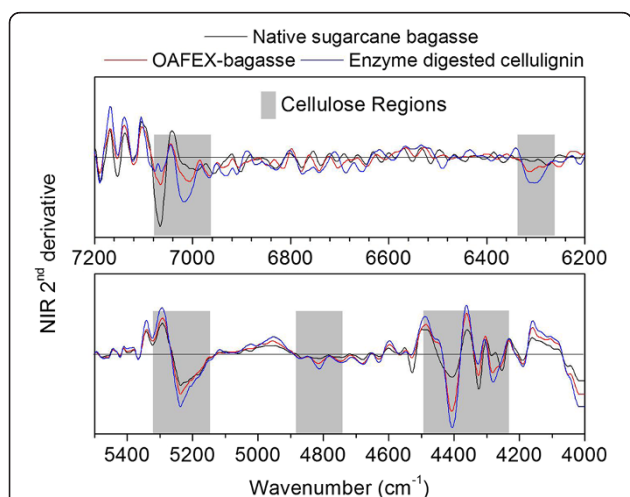
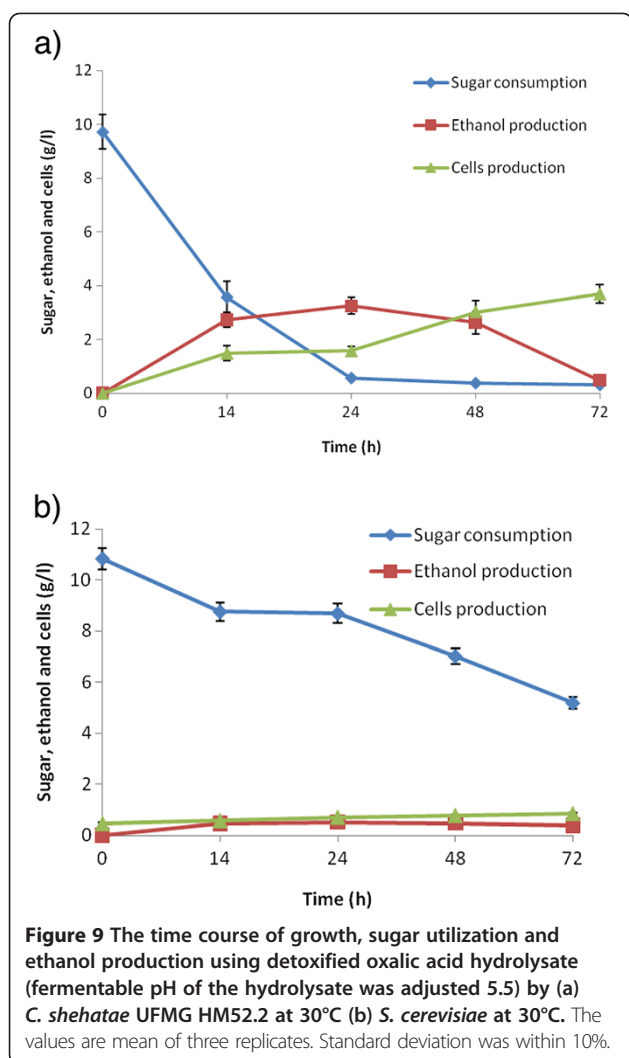


Figure 8 Second derivative of the NIR spectra (7200 to 4000 cm⁻¹) of native sugarcane bagasse (black online), pre-treated bagasse with oxalic acid (red online) and enzymatic hydrolyzed bagasse (blue online). In the OAFEX-SB, spectral region 6000 to 5920 cm⁻¹ is assigned to the C-H stretching vibration of aromatics due to the re-localization of lignin. Changes in the polysaccharide content after OAFEX and enzyme hydrolysis at regions around 6300, 5208, 4813, 4285, and 4405 cm⁻¹.



through immersing the container into running water in due course.

After hydrolysis, the hemicellulosic hydrolysate was quantitatively separated by vacuum filtration from the pretreated solids, hereinafter referred to as cellulignin. The cellulignin was thoroughly washed with deionized water and dried in oven at 45°C for 72 h, and subsequently used for enzymatic hydrolysis.

Detoxification of oxalic acid hydrolysate

OA hydrolysate was detoxified using overliming with the addition of dried calcium oxide under constant stirring until the pH reached 10.5 ± 0.05 . The fermentation inhibitors were allowed to precipitate for additional 1 h by stirring. The slurry was then subjected to vacuum filtration using Whatman filter paper #1 to remove the precipitates. The pH of clear filtrate was adjusted to 6.00 ± 0.05 with 6 N H_2SO_4 and again vacuum filtered to remove traces of salt precipitates.

Enzymatic hydrolysis

OAFEX-bagasse was enzymatically hydrolysed to depolymerise carbohydrates into simpler sugars. The OAFEX-bagasse (2 g d.wt) was pre-incubated in 40 ml of sodium citrate buffer (50 mM, pH 4.8) in 150 ml Erlenmeyer flask for 1 h at room temperature. The microbial growth was restricted by adding sodium azide (0.005%) during enzymatic hydrolysis. Soaked OAFEX-bagasse was supplemented with different cellulase loadings i.e. 20 FPU/g of the dry substrate from Celluclast 1.5 L, and 30 IU/g of β -glucosidase from Novozym 188 (Sigma-Aldrich, USA). The reaction mixture was supplemented with non-ionic surfactant (2.5 g/l, Tween-20; polyoxyethylene sorbitan monolaurate). The enzymatic hydrolysis was performed at 50°C at 150 rpm in incubator shaker (Innova 4000 Incubator Shaker, New Brunswick Scientific, Enfield, CT, USA) for 96 hrs. The samples (0.5 ml) were collected periodically (24 h), centrifuged at 5000 rpm at room temperature. The supernatant was analyzed for total reducing sugars using DNS method [49]. The extent of hydrolysis (after OA pretreatment and enzymatic hydrolysis) was calculated as follows:

Hydrolysis (%) = reducing sugar concentration obtained \times 100/Total carbohydrate content (TCC) in sugarcane bagasse.

Fermentation

Microorganisms and inoculum preparation

Microorganisms *Candida shehatae* UFMG HM 52.2 and *Saccharomyces cerevisiae* 174 were used for the fermentation of the hemicellulose hydrolysates and enzymatic hydrolysates. The microorganism *C. shehatae* UFMG HM 52.2 was isolated from a rotting-wood sample in an Atlantic Rain Forest site (Bello & Kerida Ecological Reserve) situated in the city of Nova Friburgo, Rio de Janeiro state as described by Cadete et al. [50]. *S. cerevisiae* 174 was isolated from the Atibaia river, São Paulo State, Brazil. Both microorganisms were maintained on YPD plates and stored at 4°C.

C. shehatae UFMG HM 52.2 was grown in 250 ml Erlenmeyer flasks containing 50 ml of seed medium (30 g/L of sugars (1:1 xylose and glucose), 20 g/l peptone, and 10 g/l yeast extract) in an orbital incubator shaker at 200 rpm at 30°C. Microorganism *S. cerevisiae* was grown in 250 ml Erlenmeyer flasks containing 50 ml of seed medium (30 g/l glucose, 5 g/l peptone, 3 g/l yeast extract, and 0.25 g/l Di-ammonium hydrogen phosphate) in an orbital incubator shaker at 100 rpm at 30°C for 24 h. The cultured microorganisms (*C. shehatae* and *S. cerevisiae*) were centrifuged and prepared for inoculum corresponding to 0.5 g/l cells (d. wt). The prepared inoculums were aseptically transferred into detoxified hemicellulosic and enzymatic hydrolysates (50 ml) supplemented with medium ingredients.

Ethanol fermentation

The fermentation medium (50 ml) of microorganism *C. shehatae* UFMG HM 52.2 was composed of the hydrolysates (detoxified and enzymatic) supplemented with (g/l): yeast extract (3.0), malt extract (3.0), and ammonium sulfate (5.0) at pH 5.5 [51]. In another set of fermentation, microorganism *S. cerevisiae* 174 was grown in the hydrolysates (detoxified and enzymatic) supplemented with (g/l): yeast extract (1.0), peptone (1.0), Di-ammonium hydrogen phosphate (1.0), Di-potassium hydrogen phosphate (1.0), magnesium sulfate and manganese sulfate (0.5) at pH 5.5 [24]. The hydrolysates were sterilized at 120 °C for 15 min before the use and the medium components were added aseptically prior to addition of inoculum. Fermentation reactions were setup in an orbital incubator shaker (Innova 4000 Incubator Shaker, New Brunswick Scientific, Enfield, CT, USA) at 200 rpm (*C. shehatae* UFMG HM 52.2), and 100 rpm (*S. cerevisiae* 174) for 72 h. Samples (1.0 ml) were collected periodically to determine the production of ethanol, residual sugars and formation of biomass in fermentation broth.

Analyses

The chemical composition pulverized sugarcane bagasse (native), OAFEX-SB, EH-SB was determined according to the method of Gouveia et al. [52]. Glucose, xylose, arabinose, and acetic acid, concentrations were determined by HPLC (Waters) using Biorad Aminex HPX–87H column at 45°C equipped with refraction index detector. The mobile phase was constituted with sulfuric acid 0.01 N at 0.6 mL/min flow rate as eluent. Furfural and HMF concentrations were also determined by HPLC equipped with Hewlett-Packard RP18 column and UV–VIS detector (2489) (276 nm) at 25°C. Samples were eluted by

acetonitrile/water (1:8) supplemented with 1% acetic acid (volume basis) as the eluent at a flow rate of 0.8 ml/min. Total phenolic compounds in hydrolysates were estimated calorimetrically using Folin–Ciocalteu method [53]. Ethanol production was analyzed by HPLC (Waters) using a refraction index detector (2414) and a Biorad Aminex HPX-87H column at 45°C. The growth in biomass *C. shehatae* UFMG 52.2 and *S. cerevisiae* 174 was determined at 600nm using spectrophotometer (Beckman DU640B, USA). The measured absorbance was correlated with the cell concentrations (g/l) following the calibration equation:

$$Y=2.0029x + 0.0056 \text{ (for } C. shehatae \text{ UFMG 52.2)}$$

$$Y=1.0804x + 0.006 \text{ (for } S. cerevisiae \text{ 174)}$$

Pretreatment, enzymatic hydrolysis and fermentation experiments were carried out in triplicates. The values are mean of three replicates.

Multi-scale visual analysis

Scanning electron microscope (SEM)

The SEM analysis of native, OAFEX and enzymatically hydrolysed SB was performed as described by Kristensen et al. [29]. Briefly, native, OAFEX-pretreated and enzymatically hydrolysed SB distributed on a 12 mm glass cover slip coated with poly-L-lysine (Sigma Diagnostics, S.P. Brazil). The dried sections were mounted on aluminum stubs, sputter-coated (JEOL JFC–1600) with a gold layer, and used for scanning. The prepared samples were scanned and imaged using Hitachi S520 scanning electron microscope (Hitachi, Tokyo, Japan).

Atomic force microscopy (AFM)

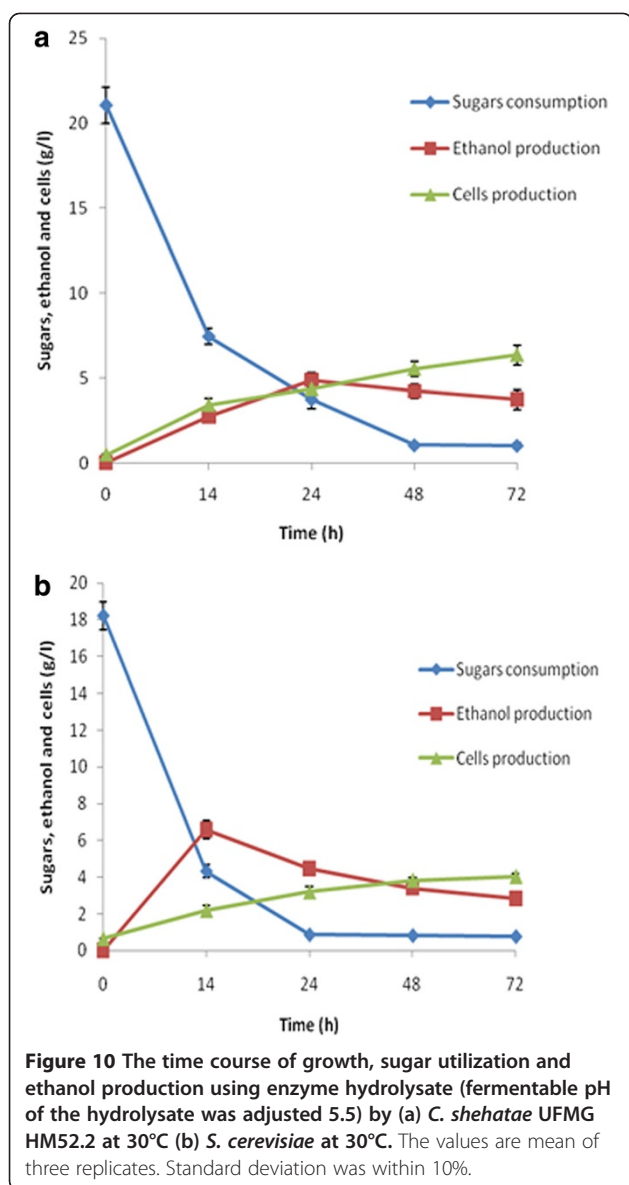
The AFM analysis of native, OA pretreated and enzymatically hydrolysed SB was performed as described by Kristensen et al. [29]. All AFM measurements were

Table 2 Kinetic parameters for ethanol production from detoxified oxalic acid hydrolysate and enzymatic hydrolysates by *Candida shehatae* UFMG HM52.2 and *Saccharomyces cerevisiae* 174

Parameters	Hemicellulose hydrolysate#		Enzyme hydrolysate##	
	<i>C. shehatae</i>	<i>S. cerevisiae</i>	<i>C. shehatae</i>	<i>S. cerevisiae</i>
Initial sugars (g/l)	9.61	10.25	21.03	18.4
Residual sugars (g/l)	0.56	8.14	3.96	0.87
Ethanol (g _p /l)	3.20	0.52	4.83	6.6
Ethanol yield (g _p /g _s)	0.353	0.246	0.282	0.46
Ethanol productivity (g _p /l/h)	0.133	0.021	0.201	0.47
Biomass (g _x /l)	3.57	0.85	6.32	4.03
Biomass yield (g _x /g _s)	0.385	0.179	0.302	0.22
Biomass productivity (g _x /l/h)	0.0496	0.011	0.0877	0.055

#During the fermentation of hemicellulosic hydrolysate by *C. shehatae* UFMG HM52.2 and *S. cerevisiae* 174, maximum ethanol was produced after 24 hrs, so ethanol productivity was calculated in both the cases considering 24 hrs. After 24 hrs of incubation, a concomitant downfall in ethanol production was observed with a regular increase in biomass. However, to calculate biomass productivities, incubation time (72 hrs) was considered.

During the fermentation of enzyme hydrolysate by *C. shehatae* UFMG HM52.2 and *S. cerevisiae* 174, maximum ethanol was produced after 24 hrs and 14 hrs respectively. Therefore ethanol productivities were calculated considering these incubation times. However biomass was found consistently increasing until the completion of fermentation (72 hrs), so biomass productivities were calculated considering 72 hrs of incubation. The values are mean of three replicates. Standard deviation was within 10%.



made with a multi-mode scanning probe microscope with a Nanoscope IIIa controller (Shimadzu SPM-9600 Deluxe, Japan). The images were acquired in tapping mode with etched silicon probe (Nanoworld Point Probe NCHR-10, 320 kHz, 42 N/m). An auto-tuning resonance frequency range of approximately 286–305 kHz with a scan rate of 0.5 Hz and sweep range of 10 kHz was used. The drive amplitude and amplitude set-point were adjusted during measurements to minimize scanning artifacts. Height, amplitude and phase images were captured simultaneously. Scan size varied from 500 nm to 5.0 μm, usually 1 μm.

Samples were fixed on metal discs with double-sided adhesive tape, and the images were measured in air. Images were collected from a minimum of 10 different fibers for each treatment with representative images

displayed in the present work. The external vibration noise was eliminated using active vibration-damping table. AFM images were recorded (512 dpi), analyzed and processed (illumination and plane fitting) by the accompanying software.

X-ray diffraction (XRD)

The crystalline nature of native, OA-treated and enzyme digested SB was analyzed by using a Scifert Isodebye Flex 3003 X-ray diffractometer (Germany). The crystallinity was analysed by adjusting the diffractometer set at 40 KV, 30 mA; radiation was Cu Kα (λ = 1.54 Å). Samples were scanned over the range of 100 <2θ <500 with a step size of 0.05° and the crystallinity index (CrI) were determined using the empirical method described by Segal et al. [54]:

$$CrI = \frac{I_{crystalline} - I_{amorphous}}{I_{crystalline}} \times 100\%$$

Where, I crystalline = intensity at 21°C and I amorphous = intensity at 18.8°C.

Raman spectroscopy

The Raman spectra of native, OA pretreated and enzyme digested SB were recorded via microRaman (T64000 Horiba Jobin Ivon, France) using the 488nm line of an argon laser, 1800 g/mm grating with a 50x objective. The samples were passed through the laser power of ~2 mW, and the scattered light were detected by a CCD system cooled with liquid nitrogen at the temperature of -130°C. To maximize the Raman signals, we have used the fact that the Raman intensity of the cellulose is dependent of the laser light polarization. Cellulose mediated polarization of laser light is dependent on the position of sample at the microscopic stage. The spectra are scaled to the cellulose peak at 1172 cm⁻¹, baseline was subtracted and smoothed with adjacent-averaging with 30 points.

Fourier transform infrared spectroscopy (FTIR)

FTIR spectroscopic analysis was performed to detect the changes in functional groups after OA pretreated and enzyme digested SB in comparison to native SB. Samples were put to mill in agate cups for 1.5 hrs with 400 rpm (RETSCH® PM 400) followed by passing through with an abronzinox sieve of 100 mesh size with an aperture of 150 μm. The pellets were prepared by mixing of 300 mg of spectroscopic grade KBr with 3 mg of sample in an agate mortar. Each sample was then submitted to 10 tons for 3 min in a hydraulic press (SPECAC 25T, ATLASTM). The spectra were collected in a VERTEX 70 spectrometer (Bruker Optics, Germany) and submitted to 4 cm⁻¹ of resolution and 72 scans per sample.

Fourier transform-Near infra-red spectroscopy (FT-NIR)

The FT-NIR spectroscopy of native, OA pretreated and enzyme digested SB samples was performed with a spectrometer FT-NIR MPA (multi-purpose analyser) from Bruker Optics, Germany. The measurements have used to diffuse reflectance which were analysed via an integrating macro sample sphere, the diameter of measured area was 15 mm, 32 scans per sample were performed with a resolution of 4 cm⁻¹ covering a range from 13000 to 3500 cm⁻¹. Second derivative spectra were calculated with 21 smoothing points after unit vector normalization. All calculations were conducted with OPUS 6.5 version software.

Competing interests

The authors declare that they have no competing interests.

Authors' contributions

AKC planned and performed the biomass pretreatment, enzymatic hydrolysis, ethanol fermentation, as well as the analysis of the results and manuscript writing. AKC also coordinated the overall study. FAFA assisted in biomass characterization, fermentation experiments and helped the manuscript drafting. VA, MJVB and LNR jointly carried out the Raman Spectroscopy, FTIR and FT-NIR analysis and written related text in the manuscript. OVS analyzed all the results and reviewed the manuscript draft. CAR and FCP provided the yeast strains and fermentation methodology. Both analyzed the fermentation results and contributed to the drafting of the text related to fermentation. SSS coordinated the overall study, analysis of results and finalizing the manuscript. All authors suggested modifications to the draft and approved the final manuscript.

Acknowledgements

Authors are grateful to FAPESP (Process n° 2008/57926-4 and 2010/11258-0) for the financial support and CNPq. FAFA gratefully acknowledges CAPES. CAR, VA, MJVB and LNR acknowledge to FAPEMIG, CNPQ and CAPES for the financial support. We are also thankful to Ms. Juliana RG Reis for her technical assistance. Authors also would like to thank Dr. Durval Rodrigues Jr., Dr. Paulo Suzuki from Engineering School of Lorena and Dr. Rogerio Hein, UNESP, Guaratingueta for SEM, XRD and AFM analysis respectively.

Author details

¹Department of Biotechnology, University of São Paulo, School of Engineering of Lorena, Estrada Municipal do Campinho- Caixa, Postal 116 12.602.810, Lorena/SP, Brazil. ²Material Spectroscopy Laboratory, Department of Physics, Federal University of Juiz de Fora, Juiz de Fora, MG 36036-330, Brazil. ³Division of Biological and Health Sciences, University of Pittsburgh Bradford, PA 16701, USA. ⁴Department of Microbiology, Federal University of Minas Gerais, Belo Horizonte, MG, Brazil. ⁵Department of Biochemistry and Microbiology, Institute of Biosciences CEIS/UNESP – Rio Claro/ SP, Brazil.

Received: 7 October 2012 Accepted: 8 January 2013

Published: 16 January 2013

References

1. Kerr RA: Energy supplies. Peak oil production may already be here. *Science* 2011, **331**:1510–1511.
2. Goldemberg J: Ethanol for a sustainable energy future. *Science* 2007, **315**:808–810.
3. Huber G, Dale BE: Grassoline at the Pump. *Sci Amer* July, 2009, 52–59.
4. Chandel AK, Silva SS, Carvalho W, Singh OV: Sugarcane bagasse and leaves: Foreseeable biomass of biofuel and bio-products. *J Chem Technol Biotechnol* 2012, **87**:11–20.
5. Himmel ME, Ding SY, Johnson DK, Adney WS, Nimlos MR, Brady JW, Foust TD: Biomass recalcitrance: engineering plants and enzymes for biofuels production. *Science* 2007, **315**:804–807.
6. Sindhu R, Binod P, Satyanagalakshmi K, Janu KU, Sajna KV, Kurien N, Sukumaran RK, Pandey A: Formic acid as a potential pretreatment agent for the conversion of sugarcane bagasse to bioethanol. *Appl Biochem Biotechnol* 2010, **162**:2313–2323.
7. Velmurugan R, Muthukumar K: Utilization of sugarcane bagasse for bioethanol production: sono-assisted acid hydrolysis approach. *Bioresour Technol* 2011, **102**:7119–7123.
8. Rezende CA, de Lima MA, Maziero P, de Azevedo ER, Garcia W, Polikarpov I: Chemical and morphological characterization of sugarcane bagasse submitted to a delignification process for enhanced enzymatic digestibility. *Biotechnol Biofuels* 2011, **4**:54.
9. Siqueira G, Milagres AMF, Carvalho W, Koch G, Ferraz A: Topochemical distribution of lignin and hydroxycinnamic acids in sugar-cane cell walls and its correlation with the enzymatic hydrolysis of polysaccharides. *Biotechnol Biofuels* 2011, **4**:7.
10. Taylor CB, Talib MF, McCabe C, Bu L, Adney WS, Himmel ME, Crowley MF, Beckham GT: Computational investigation of glycosylation effects on a family 1 carbohydrate-binding module. *J Biol Chem* 2012, **287**:3147–3155.
11. Scordia D, Cosentino SL, Lee JW, Jeffries TW: Dilute oxalic acid pretreatment for biorefining giant reed (*Arundo donax* L.). *Biomass Bioener* 2011, **35**:3018–3024.
12. Scordia D, Cosentino SL, Jeffries TW: Second generation bioethanol production from *Saccharum spontaneum* L. ssp. aegyptiacum (Willd.) Hack. *Bioresour Technol* 2010, **101**:5358–5365.
13. Lee J-W, Houtman CJ, Kim H-Y, Choi I-Y, Jeffries TW: Scale-up study of oxalic acid pretreatment of agricultural lignocellulosic biomass for the production of bioethanol. *Bioresour Technol* 2011, **102**:7451–7456.
14. Li X, Cai Z, Horn E, Winandy JE: Effect of oxalic acid pretreatment of wood chips on manufacturing medium-density fiberboard. *Holzforchung* 2011, **65**:737–741.
15. Jeffries TW: Engineering yeasts for xylose metabolism. *Curr Opin Biotechnol* 2006, **17**:320–326.
16. Chandel AK, Singh OV, Chandrasekhar G, Rao LV, Narasu ML: Key-drivers influencing the commercialization of ethanol based biorefineries. *J Comm Biotechnol* 2010, **16**:239–257.
17. Chandel AK, Kapoor RK, Singh AK, Kuhad RC: Detoxification of sugarcane bagasse hydrolysate improves ethanol production by *Candida shehatae* NCIM 3501. *Bioresour Technol* 2007, **98**:1947–1950.
18. Li Y, Park JY, Shiroma R, Ike M, Tokuyasu K: Improved ethanol and reduced xylitol production from glucose and xylose mixtures by the mutant strain of *Candida shehatae* ATCC 22984. *Appl Biochem Biotechnol* 2012, **166**:1781–1790.
19. Martín C, Galve M, Wahlbom F, Hagerdal BH, Jonsson LJ: Ethanol production from enzymatic hydrolysates of sugarcane bagasse using recombinant xylose-utilising *Saccharomyces cerevisiae*. *Enzyme Microb Technol* 2002, **31**:274–282.
20. Santos VTO, Esteves PJ, Milagres AMF, Carvalho W: Characterization of commercial cellulases and their use in the saccharification of a sugarcane bagasse sample pretreated with dilute sulfuric acid. *J Ind Microbiol Biotechnol* 2011, **38**:1089–1098.
21. Esteghlalian A, Hashimoto AG, Fenske JJ, Penner MH: Modeling and optimization of the dilute-sulfuric-acid pretreatment of corn stover, poplar and switch grass. *Bioresour Technol* 1997, **59**:129–136.
22. Rodrigues RCLB, Kenealy WR, Jeffries TW: Xylitol production from DEO hydrolysate of corn stover by *Pichia stipitis* YS-30. *J Ind Microbiol Biotechnol* 2011, **38**:1649–1655.
23. Mtui GYS: Oxalic acid pretreatment, fungal enzymatic saccharification and fermentation of maize residues to ethanol. *Afr J Biotechnol* 2011, **11**:843–851.
24. Chandel AK, Singh OV, Narasu ML, Rao LV: Bioconversion of *Saccharum spontaneum* (wild sugarcane) hemicellulosic hydrolysate into ethanol by mono and co-cultures of *Pichia stipitis* NCIM3498 and thermotolerant *Saccharomyces cerevisiae* VS₃. *New Biotechnol* 2011, **28**:593–599.
25. Chandel AK, Singh OV, Chandrasekhar G, Rao LV, Narasu ML: Bioconversion of novel substrate, *Saccharum spontaneum*, a weedy material into ethanol by *Pichia stipitis* NCIM3498. *Bioresour Technol* 2011, **102**:1709–1714.
26. Saha BC, Iten LB, Cotta MA, Wu YV: Dilute acid pretreatment, enzymatic saccharification and fermentation of wheat straw to ethanol. *Proc Biochem* 2005, **40**:3693–3700.
27. Zheng Y, Pan Z, Zhang R, Wang D: Enzymatic saccharification of dilute acid pretreated saline crops for fermentable sugar production. *Appl Ener* 2009, **86**:2459–2467.

28. Chundawat SPS, Donohoe BS, Sousa LD, Elder T, Agarwal UP, Lu FC, Ralph J, Himmel ME, Balan V, Dale BE: **Multi-scale visualization and characterization of lignocellulosic plant cell wall deconstruction during thermochemical pretreatment.** *Ener Environ Sci* 2011, **4**:973–984.
29. Kristensen JB, Thygesen LG, Felby C, Jørgensen H, Elder T: **Cell-wall structural changes in wheat straw pretreated for bioethanol production.** *Biotechnol Biofuels* 2008, **1**:5:1–9.
30. Selig MJ, Viamajala S, Decker SR, Tucker MP, Himmel ME, Vinzant TB: **Deposition of lignin droplets produced during dilute acid pretreatment of maize stems retards enzymatic hydrolysis of cellulose.** *Biotechnol Prog* 2007, **23**:1333–1339.
31. Igarashi K, Uchihashi T, Koivula A, Wada M, Kimura S, Okamoto T, Penttilä M, Ando T, Samejima M: **Traffic jams reduce hydrolytic efficiency of cellulase on cellulose surface.** *Science* 2011, **333**:1279–1282.
32. Wiley JH, Atalla RH: **Band assignments in the Raman spectra of celluloses.** *Carbohydr Res* 1987, **160**:113–129.
33. Agarwal UP, Weinstock IA, Atalla RH: **FT Raman spectroscopy for direct measurement of lignin concentrations in kraft pulps.** *Tappi J* 2003, **2**:22.
34. Ooi BG, Rambo AL, Hurtado MA: **Overcoming the recalcitrance for the conversion of Kenaf pulp to glucose via microwave-assisted pretreatment processes.** *Int J Mol Sci* 2011, **12**:1451–1463.
35. Colom X, Carrillo F, Nogués F, Garriga P: **Structural analysis of photodegraded wood by means of FTIR spectroscopy.** *Polym Degrad Stab* 2003, **80**:543–549.
36. Oh SY, Yoo D, Shin Y, Kim HC, Kim HY, Chung YS, Park WH, Youk JH: **Crystalline structure analysis of cellulose treated with sodium hydroxide and carbon dioxide by means of X-ray diffraction and FTIR spectroscopy.** *Carbohydr Res* 2005, **340**:2376–2391.
37. Pandey KK, Pitman AJ: **FTIR studies of the changes in wood chemistry following decay by brown-rot and white-rot fungi.** *Int Biodet Biodeg* 2003, **52**:151–160.
38. Pandey KK: **A study of chemical structure of soft and hardwood and wood polymers by FTIR spectroscopy.** *J Appl Polym Sci* 1999, **12**:1969–1975.
39. Kondo T: **The assignment of IR absorption bands due to free hydroxyl groups in cellulose.** *Cellulose* 1997, **4**:281–292.
40. Cao Y, Huimin T: **Structural characterization of cellulose with enzymatic treatment.** *J Mol Str* 2004, **705**:189–193.
41. Sun Y, Lin L, Deng HB, Li JZ, He BH, Sun RC: **Structural changes in Bamboo cellulose in formic acid.** *BioRes* 2008, **3**:297–315.
42. Krongtaew C, Meesner K, Ters T, Fackler K: **Qualitative NIR and pretreatment.** *BioRes* 2010, **5**:2063–2080.
43. Belini UL, Hein PRG, Filho MT, Rodrigues JC, Chaix G: **NIR for bagasse content of MDF.** *BioRes* 2011, **6**:1816–1829.
44. Inagaki T, Siesler HW, Mitsui K, Tsuchikawa S: **Crystal structure of cellulose in wood.** *Biomacromol* 2010, **11**:2300–2305.
45. Sreenath HK, Koegel RG, Moldes AB, Jeffries TW, Straub RJ: **Ethanol production from alfalfa fiber fractions by saccharification and fermentation.** *Proc Biochem* 2001, **36**:1199–1204.
46. Abbi M, Kuhad RC, Singh A: **Bioconversion of pentose sugars to ethanol by free and immobilized cells of *Candida shehatae* NCL-3501: fermentation behaviour.** *Proc Biochem* 1996, **31**:555–560.
47. Sanchez G, Pilcher L, Roslander C, Modig T, Galbe M, Liden G: **Dilute-acid hydrolysis for fermentation of the Bolivian straw material *Paja brava*.** *Bioresour Technol* 2004, **93**:249–256.
48. Sreenath HK, Jeffries TW: **Production of ethanol from wood hydrolyzates by yeasts.** *Bioresour Technol* 2000, **72**:253–260.
49. Miller GL: **Use of dinitrosalicylic acid reagent for determination of reducing sugar.** *Anal Chem* 1959, **31**:426–428.
50. Cadete RM, Melo MA, Dussán KJ, Rodrigues RC, Silva SS, Zilli JE, Vital MJ, Gomes FC, Lachance MA, Rosa CA: **Diversity and physiological characterization of D-xylose-fermenting yeasts isolated from the Brazilian amazonian forest.** *PLoS One* 2012, **7**:e43135.
51. Parekh SR, Yu S, Wayman M: **Adaptation of *Candida shehatae* and *Pichia stipitis* to wood hydrolyzates for increased ethanol production.** Aspen Bibl; 1986:Paper 3623.
52. Gouveia ER, Nascimento RT, Maior AMS, Rocha GJM: **Validação de metodologia para a caracterização química de bagaço de cana-de-açúcar.** *Quim Nova* 2009, **32**:1500–1503.
53. Scalbert A, Monties B, Janin G: **Tannins in wood: comparison of different estimation methods.** *J Agric Food Chem* 1989, **37**:1324–1329.
54. Segal L, Creely JJ, Martin AE Jr, Conrad CM: **An empirical method for estimating the degree of crystallinity of native cellulose using the X-ray diffractometer.** *Tex Res J* 1962, **29**:786–794.

doi:10.1186/1754-6834-6-4

Cite this article as: Chandel et al.: Ultra-structural mapping of sugarcane bagasse after oxalic acid fiber expansion (OAFEX) and ethanol production by *Candida shehatae* and *Saccharomyces cerevisiae*. *Biotechnology for Biofuels* 2013 **6**:4.

Submit your next manuscript to BioMed Central and take full advantage of:

- Convenient online submission
- Thorough peer review
- No space constraints or color figure charges
- Immediate publication on acceptance
- Inclusion in PubMed, CAS, Scopus and Google Scholar
- Research which is freely available for redistribution

Submit your manuscript at
www.biomedcentral.com/submit

